ELSEVIER

Time-dependent biaxial mechanical behavior of the aortic heart valve leaflet

John A. Stella, Jun Liao, Michael S. Sacks*

Engineered Tissue Mechanics Laboratory, Department of Bioengineering and the McGowan Institute for Regenerative Medicine, University of Pittsburgh, Pittsburgh, PA, USA

Abstract

Despite continued progress in the treatment of aortic valve (AV) disease, current treatments continue to be challenged to consistently restore AV function for extended durations. Improved approaches for AV repair and replacement rests upon our ability to more fully comprehend and simulate AV function. While the elastic behavior the AV leaflet (AVL) has been previously investigated, time-dependent behaviors under physiological biaxial loading states have yet to be quantified. In the current study, we performed strain rate, creep, and stress-relaxation experiments using porcine AVL under planar biaxial stretch and loaded to physiological levels (60 N/m equi-biaxial tension), with strain rates ranging from quasi-static to physiologic. The resulting stress–strain responses were found to be independent of strain rate, as was the observed low level of hysteresis (~17%). Stress relaxation and creep results indicated that while the AVL exhibited significant stress relaxation, it exhibited negligible creep over the 3 h test duration. These results are all in accordance with our previous findings for the mitral valve anterior leaflet (MVAL) [Grashow, J.S., Sacks, M.S., Liao, J., Yoganathan, A.P., 2006a. Planar biaxial creep and stress relaxatin of the mitral valve anterior leaflet. Annals of Biomedical Engineering 34 (10), 1509–1518; Grashow, J.S., Yoganathan, A.P., Sacks, M.S., 2006b. Biaxial stress-stretch behavior of the mitral valve anterior leaflet at physiologic strain rates. Annals of Biomedical Engineering 34 (2), 315–325], and support our observations that valvular tissues are *functionally* anisotropic, quasi-elastic biological materials. These results appear to be unique to valvular tissues, and indicate an ability to withstand loading without time-dependent effects under physiologic loading conditions. Based on a recent study that suggested valvular collagen fibrils are not intrinsically viscoelastic [Liao, J., Yang, L., Grashow, J., Sacks, M.S., 2007. The relation between collagen fibril kinematics and mechanical properties in the mitral valve anterior leaflet. Journal of Biomechanical Engineering 129 (1), 78–87], we speculate that the mechanisms underlying this quasi-elastic behavior may be attributed to inter-fibrillar structures unique to valvular tissues. These mechanisms are an important functional aspect of native valvular tissues, and are likely critical to improve our understanding of valvular disease and help guide the development of valvular tissue engineering and surgical repair.

1. Introduction

The aortic valve (AV) is responsible for maintaining unidirectional blood flow in response to ventricular contraction. Whether due to congenital defects or acquired degenerative maladies, it is estimated that 85,000 prosthetic valve replacements are implanted annually (AHA, 2002). Unfortunately, current surgical options for the replacement of diseased valvular tissues are not without their associated pitfalls. Pediatric applications are particularly challenging since valvular replacements are unable to adapt and grow with the individual. Mechanical implants require chronic anticoagulation therapies while bioprosthetic options have limited long-term durability.

To better establish physiological function and to establish optimal "design" attributes of an ideal valve replacement, numerous studies have been conducted to elucidate the intricate morphology and mechanical properties of the AV leaflet (AVL) (Billiar and Sacks, 2000; Lam and Sacks, 2003; Sacks, 2003; Sacks and Smith, 1998; Sacks et al., 1998; Stella and Sacks, in press; Talman and

---

*Corresponding author. Tel.: +1 412 235 5146; fax: +1 412 235 5160.
E-mail address: msacks@pitt.edu (M.S. Sacks).

Boughner, 1996; Vesely, 1998; Vesely and Noseworthy, 1992). However, due to experimental device limitations, important time-dependent behaviors have not been investigated under physiologic loading rates.

Recently, we developed a high-speed system using a planar biaxial configuration for the investigation of the mitral valve anterior leaflet (MVAL) (Grashow et al., 2006b). The MVAL was found to exhibit no strain rate sensitivity, did not creep, but did exhibit stress relaxation. In a related in vivo study of the mitral valve chordae tendoneae (Ritchie et al., 2006), it was found that the chordae exhibited a strain plateau during valve closure indicating a negligible creep response. The structural basis for these unique findings were recently explored by Liao et al. (2007) who investigated the molecular behavior of collagen via small angle X-ray scattering. Results from this study indicated that:

(a) Fibril straining did not occur until the end of the non-linear region of the tissue level stress–strain curve.
(b) Collagen fibril D-period (ε_d) increased linearly with increased tension.
(c) During creep, no changes in tissue strain or ε_d were observed.
(d) During stress relaxation, ε_d initially decayed rapidly and was followed by a slower rate of decay compared to the tissue-level stress decay rate.

These results suggested that *valvular collagen fibrils are intrinsically elastic* and are loaded only after the larger fiber structures become fully straightened. Moreover, we speculate that valvular tissues are structured at the molecular level (and probably at higher level structures as well) to achieve near-perfect elastic behaviors under physiological loading conditions. Although both valvular tissues exhibit similarities in composition and structure, the AVL is geometrically, structurally, and biomechanically unique. Thus, the objective of the current study was to quantify the time-dependent behaviors of the native AVL under dynamic physiological loading conditions.

2. Methods

2.1. Tissue preparation

Porcine AVLs were prepared from fresh aortic roots and snap frozen at −80 °C. Based on previous studies, short-term low-temperature storage has been shown to induce minimal effects on connective tissue mechanical behavior (Woo et al., 1994). Preceeding testing, leaflets were thawed in a 37 °C water bath and a specimen was cut from the central lower belly region measuring approximately 9 mm × 6 mm in the circumferential and radial directions, respectively. A total of eight specimens were prepared for each of the three testing groups (see below).

2.2. Mechanical testing

A complete description of the biaxial testing device has been recently presented (Grashow et al., 2006a, b). A maximum equi-biaxial membrane tension of 60 N/m was utilized, with strains referenced to a precondi-

tioned, free-floating configuration. To evaluate stretch rate sensitivity, preconditioned specimens were loaded to a maximum membrane tension of 60 N/m and unloaded in half cycle times of 1, 0.5, 0.1, 0.05 s with the peak equi-biaxial tension of 60 N/m chosen based on in vivo diastolic pressures (Thubrikar, 1990), as well as a physiologic stress of ~240 kPa (Cataloglu et al., 1977) for an assumed thickness of 500 µm. As in our mitral valve study, hysteresis was quantified from the tension–areal stretch response, which represents the total tissue membrane strain energy (Fig. 3). To assess planar biaxial relaxation and creep, the specimens for these two groups were preconditioned to the maximum membrane tension of 60 N/m and followed by either creep or relaxation tests with a rise time of 100 ms.

While we were able to consistently obtain excellent loading data, unavoidable water bath vibrations present during the 0.05 s unloading phase prevented us from obtaining accurate unloading data. It should be noted that these were not due to device loading frame vibrations but from fluid currents in the bath. Qualitatively, there were no observable differences from the other test groups but the hysteresis measurements for the 0.05 s loading group have been excluded.

2.3. Statistical analysis

Stress and stretch results were expressed as mean ± standard error of the mean (SEM), with differences considered statistically significant when $p < 0.05$. To determine the effects of stretch rate on the observed peak stretch and hysteresis, comparisons between all loading times were performed using one-way repeated measures analysis of variance (ANOVA). For all tests, the circumferential and radial data groups were considered separately. One-way ANOVA tests were also used to assess any directional differences between specimen axes in both creep and relaxation experiments over the length of the test (100 ms, 300 ms, 1 s, and 3 h). All statistics were performed with a commercial software package (SigmaStat; SPSS Inc., Chicago, IL).

3. Results

3.1. Effects of strain rate on AV tissue response

The biaxial testing device was capable of replicating physiologic stretch rates for the AVL (Table 1) and the

Table 1
The stretch and strain rate values measured during testing, with biaxial strain rates ranging from quasi-static to physiologic, reported as the mean ± SEM

Half cycle time	Stretch		Strain rate (%/s)	
	Circular	Radial	Circular	Radial
15 s	1.18 ± 0.02	1.57 ± 0.06	1.2 ± 0.14	3.8 ± 0.40
1 s	1.19 ± 0.02	1.64 ± 0.03	19.5 ± 1.85	63.96 ± 2.63
0.5 s	1.19 ± 0.02	1.63 ± 0.03	37.8 ± 3.61	126.83 ± 5.26
0.1 s	1.19 ± 0.02	1.63 ± 0.04	185.9 ± 20.1	630.9 ± 25.7
0.05 s	1.19 ± 0.02	1.59 ± 0.03	381.0 ± 47.2	1183.8 ± 51.3
In vivo (Thubrikar, 1990)	1.11 ± 0.02	1.31 ± 0.04	440 ± 80.0	1240 ± 160.0

For comparison, previously reported in vivo stretch and strain rate data from Thubrikar (1990), who utilized a canine model and high-speed imaging to measure in vivo leaflet uni-dimensional strain rates throughout the cardiac cycle. Note that the shortest loading time of 0.05 s produced peak stretches and strain rates comparable to those measured in vivo, suggesting that the current study was able to produce physiological strain rates.

resulting shapes of the tension vs. stretch loading curves were very similar (Fig. 1). Overall, the tension–stretch behaviors exhibited in the current study were in close agreement with previously reported biaxial behaviors for native AV tissues, including the mean peak stretch values (Billiar and Sacks, 2000; Stella and Sacks, in press). In addition, no measurable strain rate effects were observed (Fig. 1a) and the testing device exhibited high repeatability (Fig. 1b). To better present the strain rate effects, mean peak stretches (λ_{peak}^c, λ_{peak}^r) for each cycle period were pooled (Fig. 2). No significant differences were found between any of the loading time protocols in both the circumferential ($p = 0.821$) and radial ($p = 0.486$) directions. Although the MVAL exhibited a stiffer response in the radial direction than the AVL, peak stretches in the circumferential and radial directions were not dependent upon the rate of stretch (Fig. 2b).

3.2. Effects of strain rate on hysteresis

In the hysteresis responses along the circumferential and radial directions, we consistently observed no detectable hysteresis in the circumferential direction and a small amount in the radial direction for all strain rates. Examination of the tension–areal stretch response suggests no significant difference in membrane strain energy between the various strain rate groups ($p = 0.342$). Although levels of strain energy differed for the AVL compared to the MVAL, both tissues exhibited a strain rate-independent hysteresis response (Fig. 3c–d).
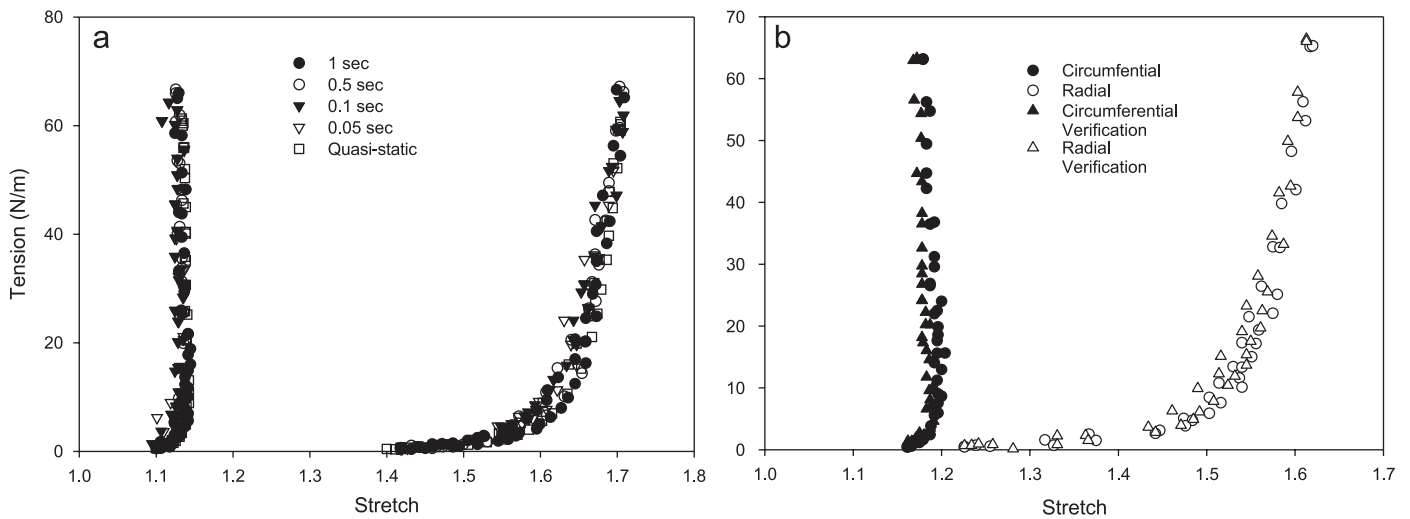

Fig. 1. (a) Representative AV loading and unloading curves during 15, 1, 0.5, 0.1, and 0.05 s half cycle times. Results indicate consistent tension–stretch responses for all protocols and no observable stretch rate sensitivity. (b) To quantify test repeatability, the initial 1.0 s half-cycle protocol was compared to an additional protocol performed after testing. High levels of repeatability indicate that the biaxial device is capable of accurately controlling high strain rate tests while not causing tissue damage.
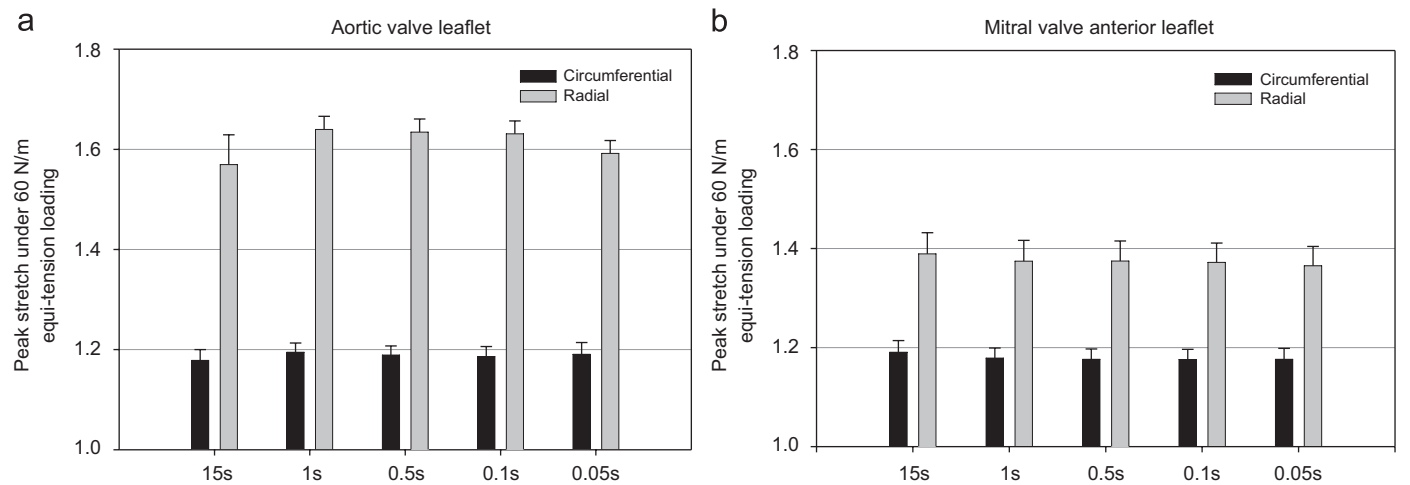

Fig. 2. (a) Averaged AVL peak stretch behavior ($n = 8$). Circumferential and radial peak stretch is significantly different while peak stretches at the 60 N/m equi-biaxial tension state revealed no significant differences for any loading time ($p = 0.821$ and $p = 0.486$ for the circumferential and radial peak stretch, respectively). These results support the observation that AVL tension is independent of the rate of stretch. (b) Similarly, the mitral valve anterior leaflet exhibited peak stretch rate independence.
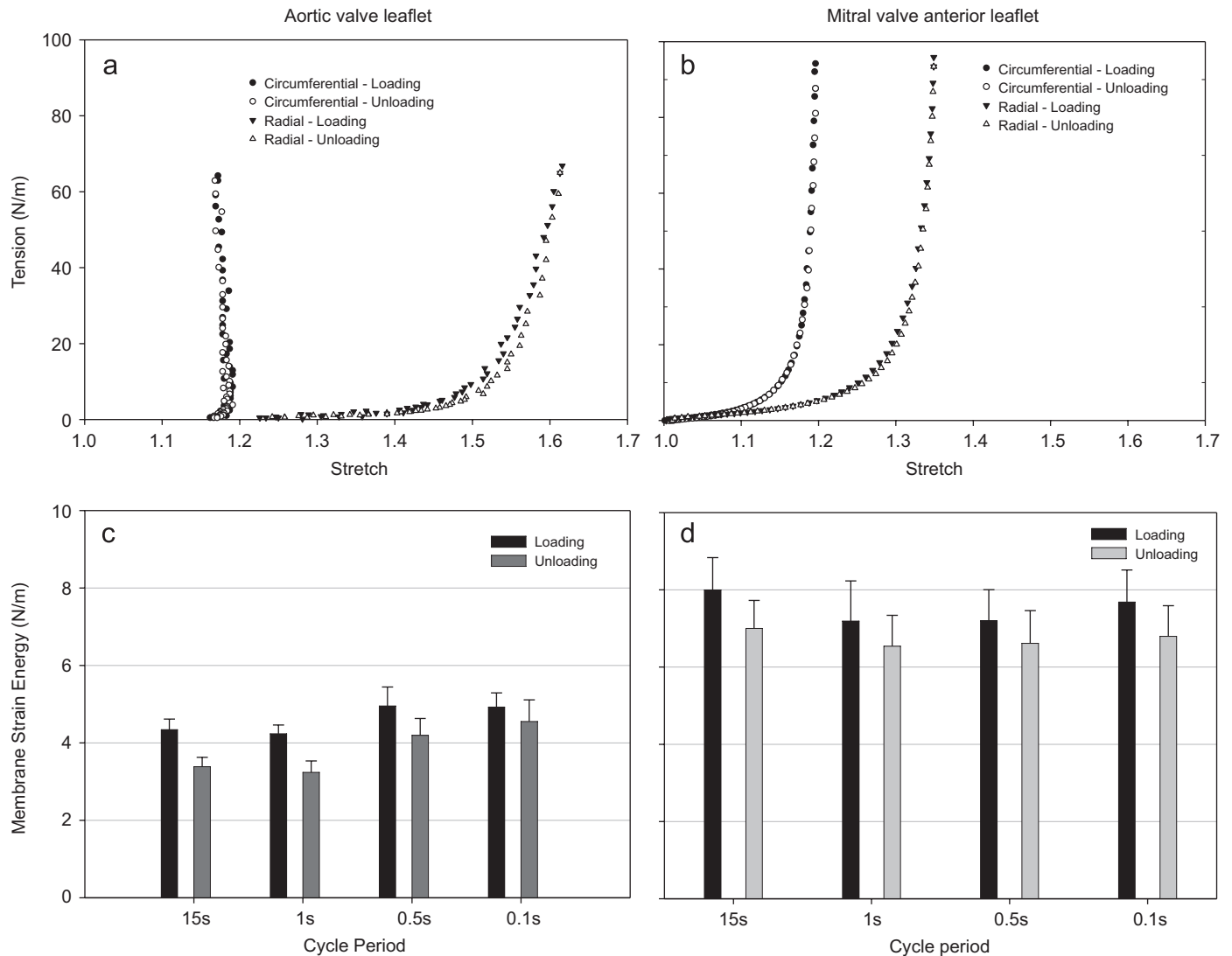
Fig. 3. Representative loading and unloading curves for the (a) AV and the (b) MVAL depicting minimal energy loss. Mean (c) AV and (d) MVAL energy storage and dissipation for all stretch rates. Hysteresis is defined as the area under tension–areal stretch curve. This definition was utilized as it represents the total tissue membrane strain energy in units of N/m. Half-cycle time (0.05 s) is not presented due to unavoidable fluid currents during the unloading phase. AV hysteresis changes due to increased strain rate were not significantly different (loading: $p = 0.342$; unloading: $p = 0.083$; change in energy: $p = 0.387$).

3.3. Biaxial stress relaxation

For stress relaxation, peak stretches were maintained to within $\pm 0.1\%$ strain over the entire 3 h test period. Substantial stress relaxation was observed in both the circumferential and radial directions. Initially (first 20 min), rapid relaxation was observed and was followed by continually slowing relaxation (Fig. 4a). Quantitatively, the relaxation percentage in the circumferential direction $(27.51 \pm 1.07\%)$ was statistically different $(p = 0.007)$ from the radial direction $(33.28 \pm 1.35\%)$. Although the AV tended to exhibit more relaxation, it was not significantly different from the MVAL values of $24.67 \pm 0.93\%$ and $32.09 \pm 0.77\%$ in the circumferential and radial directions, respectively (Fig. 4b).

3.4. Biaxial creep response

The high degree of mechanical anisotropy as reported previously (Billiar and Sacks, 2000; Lo and Vesely, 1995; Missirlis and Chong, 1978; Sauren et al., 1983; Thubrikar, 1990; Vesely and Noseworthy, 1992) was observed in the creep experiments (Fig. 5a). Specifically, peak stretches at the 300 ms time point were 1.04 ± 0.026 in the circumferential direction and 1.43 ± 0.067 in the radial direction (Fig. 5b). In sharp contrast to the relaxation studies, the observed creep was negligible in both the circumferential and radial specimen axes for the entire test duration (Fig. 5b). Mean stretches in the circumferential and radial directions indicated no significant differences between the creep stretch levels at different loading durations
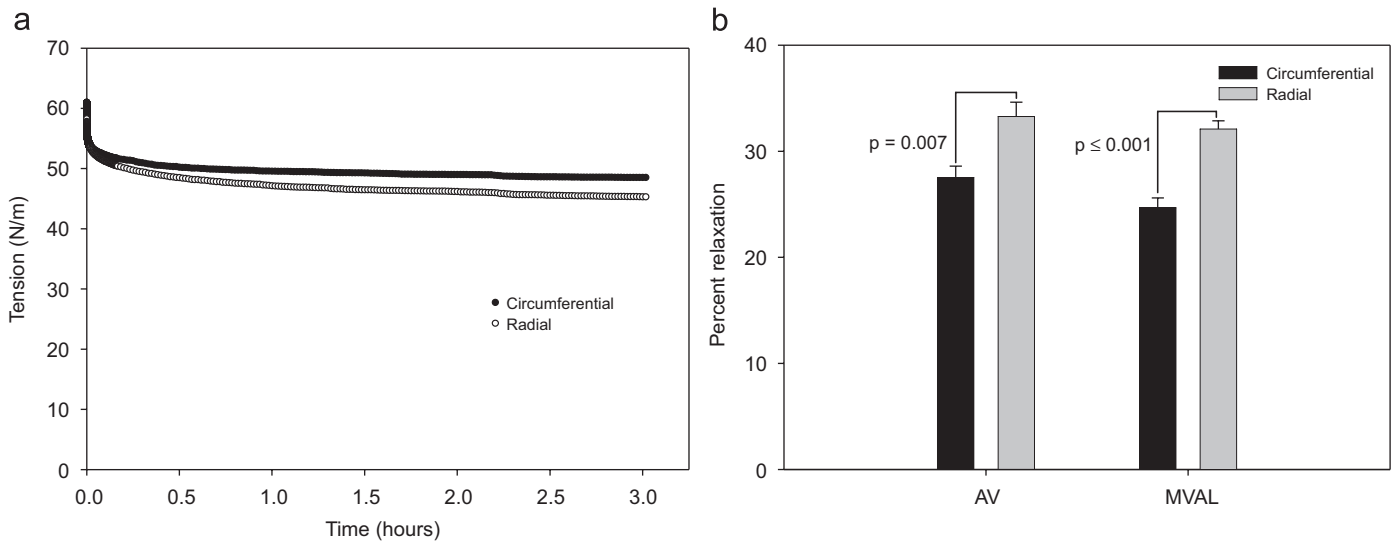
Fig. 4. (a) Representative stress-relaxation behavior of the AVL. (b) Percent relaxation at 3 h for the AV ($n = 6$) and MVAL biaxial stress-relaxation behavior. The observed AV relaxation in the circumferential direction was statistically different from the radial relaxation response ($p = 0.007$). The AVL exhibited comparable levels of relaxation in both the circumferential and radial directions to the MVAL that were not statically significant (circumferential: $p = 0.068$; radial: $p = 0.431$).
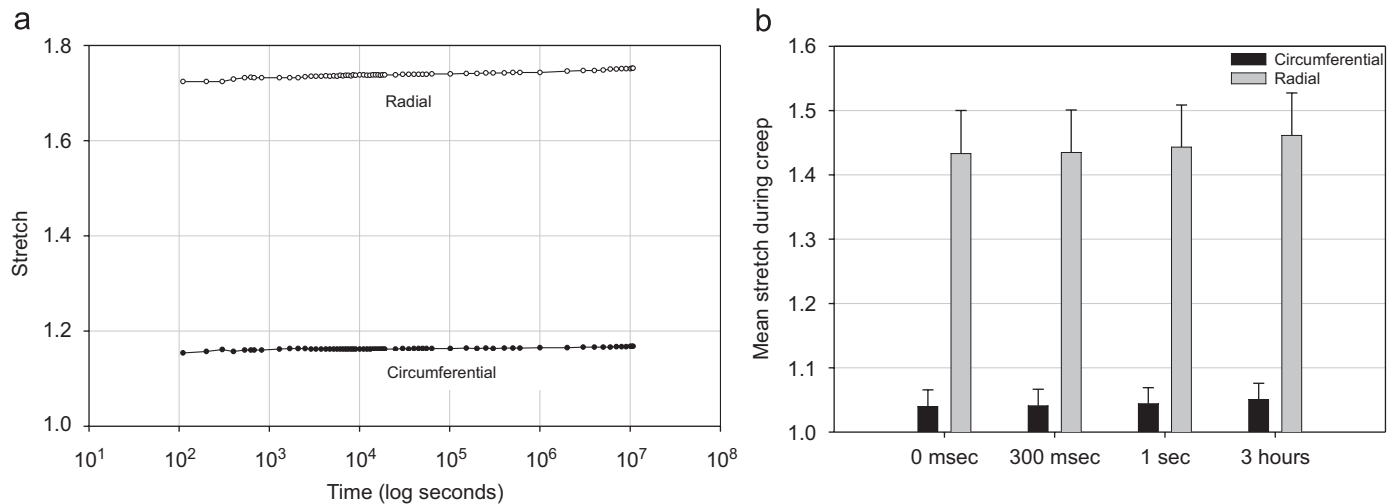

Fig. 5. (a) Representative AV planar biaxial creep behavior for the circumferential and radial directions over the 3 h test. The highly anisotropic behavior of the AVL was clearly observable. (b) The mean stretch observed during creep tests ($n = 6$), indicating that creep in both the circumferential and radial axes, was negligible for all time points.

(0 ms, 300 ms, 1 s, and 3 h) on either the circumferential ($p = 0.821$) or radial ($p = 0.486$) axes (Fig. 5b).

4. Discussion

Traditionally, modeling the time-dependent response of anisotropic non-linear viscoelastic biological tissues such as the AVL has most often utilized the quasi-linear viscoelastic (QLV) approach (Fung, 1993). This approach assumes that the tissues time-dependent mechanical properties are all manifestations of the same underlying physical mechanism, mathematically idealized as a continuous spectrum. The underlying physical mechanisms for the observed viscoelastic behavior may include collagen fibril–fibril interactions (Liao and Vesely, 2004) or intrinsic collagen viscoelasticity. If these assumptions hold, both creep and relaxation behaviors should in theory be derivable from each other (Wineman and Rajagopal, 2000).

However, Thornton et al. (1997) observed a disparity between the rate of relaxation and creep at low stress levels and further demonstrated that ligament creep could not be predicted from relaxation data utilizing QLV theory. Mechanistically, it was shown that ligament creep was a fiber recruitment-mediated behavior (Thornton et al., 2001). In a related study, Provenzano et al. (2001) observed the rate of creep and relaxation to be dependent upon initial stress and strain levels, respectively, and that the rate

of relaxation proceeded faster than the rate of creep in contra-lateral ligaments initiating the authors to suggest a more general approach than QLV theory to appropriately describe the non-linear viscoelastic behavior of rat medial collateral ligament.

Our findings clearly indicate that the mechanisms responsible for creep and relaxation in the AVL are *functionally independent*. As in our recent MVAL studies (Grashow et al., 2006a, 2006b; Liao et al., 2007), the AVL does not conform to viscoelastic material definitions under planar biaxial loading states. Instead, we believe it more appropriate to describe valvular tissues as *quasi-elastic*. That is to say, valvular tissues exhibit the following unique mechanical properties:

(a) Capable of undergoing large, rapid anisotropic strains in response to the transvalvular pressure gradients and returning to their original configuration when un-loaded.
(b) No measurable creep under physiologically relevant loading conditions.
(c) Small viscous dissipative effects (hysteresis).
(d) Substantial, directionally dependent stress relaxation.

Our results suggest that it is not necessary to develop models of time-dependent behavior for organ-level simulations of valve function. Rather, it is more relevant to focus on how valvular tissues achieve their unique mechanical responses and how it may be altered in diseased states.

4.1. Physiological loading, strain levels, and strain rates

The range of strain rates utilized in the present study was chosen such that they encompass strain rates from quasi-static to physiologic. These strain rate values were based on previous studies (Thubrikar, 1990) of canine leaflet motion during the cardiac cycle and strains exhibited during normal transvalvular pressures. Specifically, three radiopaque markers were placed on the leaflet in the radial or circumferential direction. From the mid-diastole reference configuration, displacement of the circumferentially and radially oriented markers could be obtained throughout the cardiac cycle. Also, radiopaque markers attached to the leaflet surface were used to quantify leaflet deformation in response to transvalvular pressure. In vivo strains of 10.1% and 30.8% in the circumferential and radial directions, respectively, were reported during valve closure over a period of approximately 20–25 ms. From these in vivo measurements, the corresponding circumferential and radial strain rates are $440 \pm 80.0\%$/s and $1240 \pm 160.0\%$/s, respectively. In the current study, the maximum circumferential and radial strain rates obtained were $381.0 \pm 47.2\%$/s and $1183.8 \pm 51.3\%$/s, respectively. Although subtle variations between species are likely, it is reasonably to assume that comparable strain rates would be observed. Based upon this limited experimental data, the high-speed biaxial

testing device employed for the current study was capable of replicating in vivo strain rates.

When relating the current study to valve function, it is interesting to note that the stress–strain behavior of the AVL and MVAL was independent of stretch rate along both stretch axes (Figs. 2 and 3) (Grashow et al., 2006b). Similarly, Naimark et al. (1992) showed no significant strain rate dependence in the stress–strain relationship of mammalian pericardia for strain rates between 1%/s and 100%/s. The authors speculated that strain rate insensitivity may be attributed to the stabilizing effects of glycosaminoglycans that surround the pericardial collagen fibers. Despite these similarities, some inconsistencies do arise throughout the literature. Leeson-Dietrich et al. (1995) found significant differences in the stress–strain response at different strain rates of both the aortic and pulmonary heart valves. Potential explanations for these disparities could be attributed to subtle structural differences or arise from varied modes of deformation (uniaxial vs. biaxial).

4.2. Stress relaxation

Despite exhibiting a relaxation response qualitatively similar to other collagenous soft tissues, AVL relaxation was observed to be directionally dependent. This discrepancy is likely a result of structural anisotropy wherein collagen fibers are required to rotate toward the radial axis during equi-biaxial loading conditions and may induce altered fiber level interactions. Given the lack of strain rate sensitivity, differences in the relaxation behavior would not be associated with the different strain rates required to obtain the 60 N/m equi-biaxial tension state.

4.3. Creep relationship to stress relaxation

While the AVL exhibited relaxation, no measurable degree of creep was observed over the 3 h test duration (Fig. 5). This behavior was observed in the MVAL (Grashow et al., 2006a), but was inconsistent with findings for ligament (Provenzano et al., 2001; Thornton et al., 1997) and pericardium (Lee and Boughner, 1985). It is important to note that the uniaxial testing methods employed in the pericardium studies may account for some of the disparities observed in creep behaviors. For example, uniaxial loading conditions impart altered microstructural kinematics (i.e., collagen fiber rotations) than those exhibited during multiaxial loading conditions owing to multiple apparent behaviors from the same material (Gilbert et al., 2006). In uniaxial creep testing, the unconstrained specimen edges orthogonal to the direction of deformation may allow fibers the potential to rotate in a time-dependent manner to achieve a state of reduced fiber stress. Conversely, there are no unconstrained segments of the specimen during biaxial creep testing owing to a lack of time-dependent changes in fiber orientation. Moreover, in a related in vivo study (Ritchie et al., 2006), it was found

that mitral valve chordae tendinae exhibit a strain plateau during valve closure and no observable creep. This result is consistent with our MVAL small angle X-ray studies (Liao et al., 2007). Taken as a whole, it appears that while valvular tissues can exhibit stress relaxation, they do not exhibit any creep-like behaviors under physiological loading.

4.4. Potential effects of regional variations in the AVL

It has been well established that the AVL exhibits significant regional variations in mechanical behavior with respect to strains measured in the intact belly region (Adamczyk and Vesely, 2002a, b) and biaxial mechanical properties measured in the central coaptation region under planar biaxial stretch (Billiar and Sacks, 2000). Currently, experimental studies evaluating commissure region properties are limited to the flexural properties (Mirnajafi et al., 2006). It was noted that, consistent with previous studies (Thubrikar, 1990), the commissure region was composed of dense collagenous fibers with no observable spongiosa layer nor rich in observable GAGs. Conversely, the belly region is the only part of the AVL rich in highly viscous GAGs (Schoen, 2005), and is thus most likely to exhibit viscoelastic behavior. Thus, while profound regional variations in AVL mechanical properties exist, the quasi-elastic behavior of the AVL belly region likely represents an upper bound to tensile viscoelastic behavior.

4.5. Insight into underlying structural mechanisms

As mentioned previously, in the MVAL (Liao et al., 2007), the decrease in collagen fibril D-period during stress relaxation correlated well to the stress decay, albeit with a different time constant. However, the collagen fibril D-period remained constant while the tissue was exposed to a constant stress. This D-period behavior under constant stress was also exhibited in the rat tail tendon, and tissue-level creep was attributed to fibrillar slippage (Folkhard et al., 1987). It has been documented that collagen fibrils are discontinuous and adjacent fibrils are linked via orthogonally oriented proteoglycans (Liao et al., 2007; Redalli et al., 2003). These proteoglycans tend to rotate in the direction of tissue deformation and could contribute mechanically at large strains (Liao et al., 2007). These interactions may play a role during constant strain states whereby the energy stored in stiff collagen fibers is transferred to the proteoglycan bridges or other ECM structures, enabling the collagen fibers to attain a lower-energy state. However, during constant stress conditions, the collagen fibers are unable to transfer energy to the surrounding matrix as they are responsible for balancing the externally applied tractions. In addition, the lack of valvular tissue-level creep could also indicate that the strength and number of fibril–ECM interactions (e.g., proteoglycan–collagen interactions) vary between tissues.

Based on these findings, we speculate that the unique valvular tissue quasi-elastic behavior is a function of the mechanical interactions *between* the constituent collagen fibrils and the surrounding matrix.

To gain better insight into these mechanisms, we utilized a transmission electron microscopy (TEM) technique developed by Haigh and Scott (1986). This procedure involves the use of Cuperomeronic Blue and the critical electrolyte concentration technique to stain proteoglycans. We observed abundant proteoglycans in all layers of the AVL (Fig. 6). In the fibrosa layer specifically, small proteoglycans (decorin) were found to mechanically interact with collagen fibrils via specific binding to the collagen D-period (Fig. 6a). These abundant interactions may lead to tissue-level viscoelastic behavior under non-physiological conditions (i.e., stress relaxation) while the collagen fibril itself is intrinsically elastic.

4.6. Relation to valvular function

Although the structural mechanisms underlying the time-dependent behavior of the AVL are complex, its functional basis is straightforward and intuitive. Namely, the ability to primarily exhibit an elastic behavior while demonstrating the capability to dramatically stiffen at physiologic loading levels is highly desirable. Interestingly, while valvular tissues are composed of typical load bearing soft-tissue constituents (e.g., collagen type I, GAGs, elastin), they clearly exhibit functionally unique behaviors. Moreover, while the exact structural mechanisms remain uncertain, they clearly warrant further investigation as they may have important implications related to degenerative valve disease (Schoen, 2005) as well as developing engineered valvular tissues in vivo (Sutherland et al., 2005).

4.7. Limitations

The current study experienced limitations similar to those previously reported by Grashow et al. for the MVAL leaflet (Grashow et al., 2006a, b). It is also important to note that differences likely exist between the non-, right-, and left-coronary leaflets (Adamczyk and Vesely, 2002a, b; Lo and Vesely, 1995). Also, we did not examine the potential differences between species (Mohri et al., 1972). However, given the consistency in overall physiological function, it is likely that the results presented herein for the porcine AVL are representative.

4.8. Conclusions

The results from the present study for the AVL and our previous MVAL studies support our observation that valvular tissues functionally behave as anisotropic quasi-elastic materials. These results appear to be unique to valvular tissues and indicate an ability to withstand loading without time-dependent effects under physiologic loading conditions. We speculate that degenerated ECM
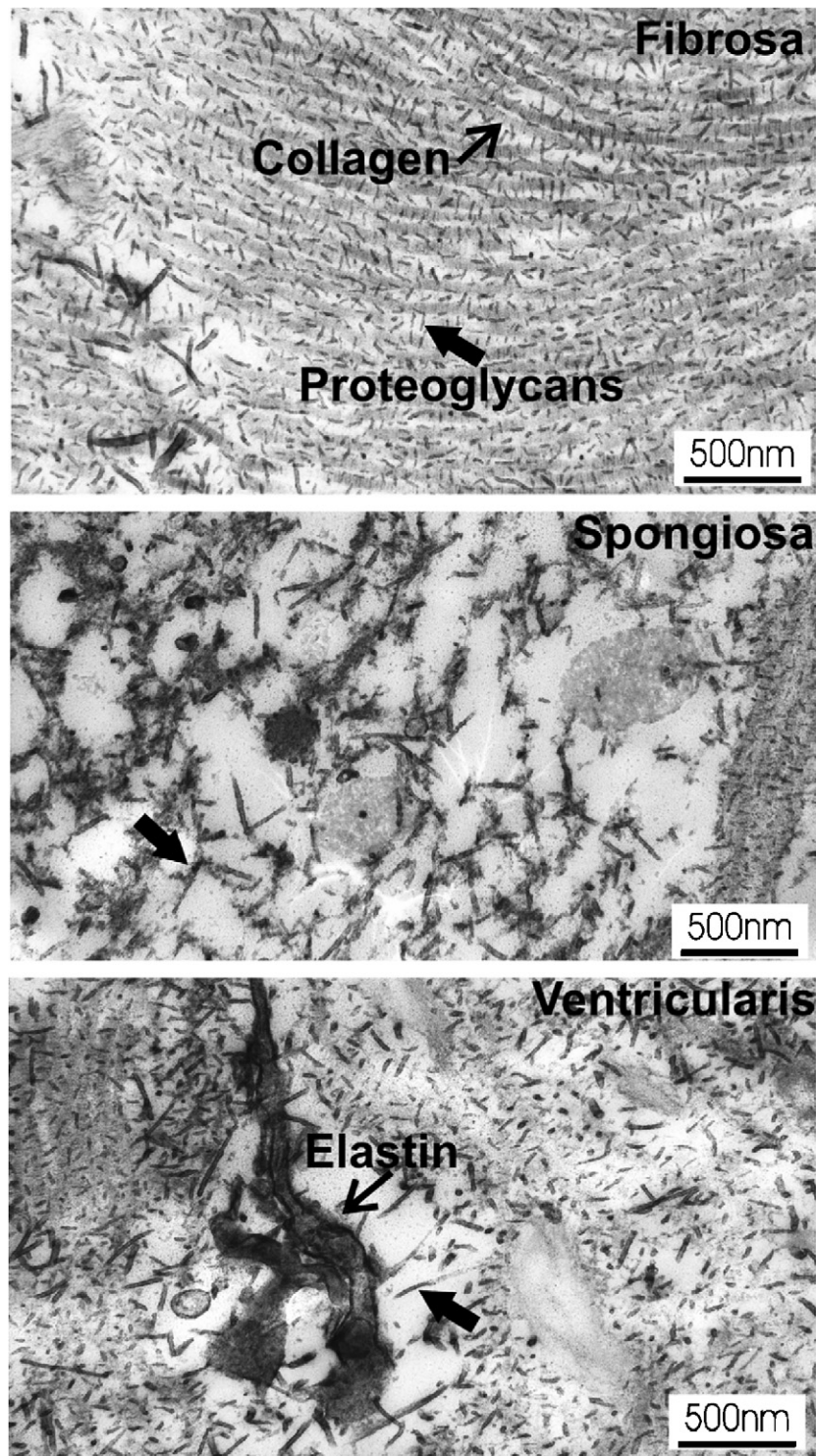
Fig. 6. Ultrastructural interaction in fibrosa, spongiosa, and ventricularis layers revealed with TEM and Cuperomeronic Blue staining. The image shows proteoglycans, marked with solid dark arrows, interacting with ECM components such as collagen fibers. It is our hypothesis that intricate interactions between collagen and other ECM components, such as proteoglycans, significantly contribute to the unique time-dependent material properties exhibited by valvular tissues.

components in diseased AV might induce changes in these quasi-elastic behaviors, leading to valvular deterioration. Moreover, these subtle tissue behaviors could prove critical to the development of tissue-engineered alternatives for valve repair or replacement.

References

Adamczyk, M.M., Vesely, I., 2002a. Biaxial strain distributions in explanted porcine bioprosthetic valves. Journal of Heart Valve Disease 11 (5), 688–695.

Adamczyk, M.M., Vesely, I., 2002b. Characteristics of compressive strains in porcine aortic valves cusps. Journal of Heart Valve Disease 11 (1), 75–83.

AHA, 2002. Heart Disease and Stroke Statistics—2003 Update. American Heart Association, Dallas, TX.

Billiar, K.L., Sacks, M.S., 2000. Biaxial mechanical properties of the natural and glutaraldehyde treated aortic valve cusp—Part I: experimental results. Journal of Biomechanical Engineering 122 (1), 23–30.

Cataloglu, A., Clark, R.E., Gould, P.L., 1977. Stress analysis of aortic valve leaflets with smoothed geometrical data. Journal of Biomechanics 10, 153–158.

Folkhard, W., Geercken, W., Knorzer, E., Mosler, E., Nemetschek-Gansler, H., Nemetschek, T., Koch, M.H., 1987. Structural dynamic of native tendon collagen. Journal of Molecular Biology 193 (2), 405–407.

Fung, Y.C., 1993. Biomechanics: Mechanical Properties of Living Tissues. Springer, New York.

Gilbert, T.W., Sacks, M.S., Grashow, J.S., Woo, S.L., Badylak, S.F., Chancellor, M.B., 2006. Fiber kinematics of small intestinal submucosa under biaxial and uniaxial stretch. Journal of Biomechanical Engineering 128 (6), 890–898.

Grashow, J.S., Sacks, M.S., Liao, J., Yoganathan, A.P., 2006a. Planar biaxial creep and stress relaxation of the mitral valve anterior leaflet. Annals of Biomedical Engineering 34 (10), 1509–1518.

Grashow, J.S., Yoganathan, A.P., Sacks, M.S., 2006b. Biaxial stress-stretch behavior of the mitral valve anterior leaflet at physiologic strain rates. Annals of Biomedical Engineering 34 (2), 315–325.

Haigh, M., Scott, J.E., 1986. A method of processing tissue sections for staining with cu-promeronic blue and other dyes, using CEC techniques, for light and electron microscopy. Basic Applications of Histochemistry 30 (4), 479–486.

Lam, T.V., Sacks, M.S., 2003. Transmural strains of heart valve tissues under flexure. Annual Biomedical Engineering Society Fall Meeting, Nashville, TN.

Lee, J.M., Boughner, D.R., 1985. Mechanical properties of human pericardium. Differences in viscoelastic response when compared with canine pericardium. Circulation Research 57 (3), 475–481.

Leeson-Dietrich, J., Boughner, D., Vesely, I., 1995. Porcine pulmonary and aortic valves: a comparison of their tensile viscoelastic properties at physiological strain rates. The Journal of Heart Valve Disease 4, 88–94.

Liao, J., Vesely, I., 2004. Relationship between collagen fibrils, glycosaminoglycans, and stress relaxation in mitral valve chordae tendineae. Annals of Biomedical Engineering 32 (7), 977–983.

Liao, J., Yang, L., Grashow, J., Sacks, M.S., 2007. The relation between collagen fibril kinematics and mechanical properties in the mitral valve anterior leaflet. Journal of Biomechanical Engineering 129 (1), 78–87.

Lo, D., Vesely, I., 1995. Biaxial strain analysis of the porcine aortic valve. Annals of Thoracic Surgery 60, S374–S378.

Mirnajafi, A., Raymer, J.M., McClure, L.R., Sacks, M.S., 2006. The flexural rigidity of the aortic valve leaflet in the commissural region. Journal of Biomechanics 39 (16), 2966–2973.

Missirlis, Y., Chong, M., 1978. Aortic valve mechanics—part I: material properties of natural porcine aortic vavles. Journal of Bioengineering 2, 287–300.

Mohri, H., Reichenback, D., Merendino, K., 1972. Biology of homologous and heterologous aortic valves. In: Ionescu, M., Ross, D., Wooler, G. (Eds.), Biological Tissue in Heart Valve Replacement. Butterworths, London, p. 137.

Naimark, W.A., Lee, J.M., Limeback, H., Cheung, D., 1992. Correlation of structure and viscoelastic properties in the pericardia of four mammalian species. American Journal of Physiology 263 (32), H1095–H1106.

Provenzano, P., Lakes, R., Keenan, T., Vanderby Jr., R., 2001. Nonlinear ligament viscoelasticity. Annals of Biomedical Engineering 29 (10), 908–914.

Redalli, A., Vesentini, S., Soncini, M., Vena, P., Mantero, S., Montevecchi, F.M., 2003. Possible role of decorin glycosaminoglycans in fibril to fibril force transfer in relative mature tendons—a computational study from molecular to microstructural level. Journal of Biomechanics 36, 1555–1569.

Ritchie, J., Jimenez, J., He, Z., Sacks, M.S., Yoganathan, A.P., 2006. The material properties of the native porcine mitral valve chordae tendineae: an in vitro investigation. Journal of Biomechanics 39 (6), 1129–1135.

Sacks, M.S., 2003. Biomechanics of native and engineered heart valve tissues. In: Guilak, F., Butler, D.L., Goldstein, S., Mooney, D. (Eds.), Functional Tissue Engineering. Springer, New York.

Sacks, M.S., Smith, D.B., 1998. Effects of accelerated testing on porcine bioprosthetic heart valve fiber architecture. Biomaterials 19 (11–12), 1027–1036.

Sacks, M.S., Smith, D.B., Hiester, E.D., 1998. The aortic valve microstructure: effects of transvalvular pressure. Journal of Biomedical Materials Research 41 (1), 131–141.

Sauren, A.A., van Hout, M.C., van Steenhoven, A.A., Veldpaus, F.E., Janssen, J.D., 1983. The mechanical properties of porcine aortic valve tissues. Journal of Biomechanics 16 (5), 327–337.

Schoen, F.J., 2005. Cardiac valves and valvular pathology: update on function, disease, repair, and replacement. Cardiovascular Pathology 14 (4), 189–194.

Stella, J., Sacks, M.S., in press. On the biaxial mechanical properties of the layers of the aortic valve leaflet. Journal of Biomechanical Engineering.

Sutherland, F.W., Perry, T.E., Yu, Y., Sherwood, M.C., Rabkin, E., Masuda, Y., et al., 2005. From stem cells to viable autologous semilunar heart valve. Circulation 111 (21), 2783–2791.

Talman, E., Boughner, D., 1996. Internal shear properties of fresh aortic valve cusps: implications for normal valve function. Journal of Heart Valve Disease 5, 152–159.

Thornton, G.M., Oliynyk, A., Frank, C.B., Shrive, N.G., 1997. Ligament creep cannot be predicted from stress relaxation at low stress: a biomechanical study of the rabbit medial collateral ligament. Journal of Orthopaedic Research 15 (5), 652–656.

Thornton, G.M., Frank, C.B., Shrive, N.G., 2001. Ligament creep behavior can be predicted from stress relaxation by incorporating fiber recruitment. Journal of Rheology 45 (2), 493–507.

Thubrikar, M., 1990. The Aortic Valve. CRC, Boca Raton.

Vesely, I., 1998. The role of elastin in aortic valve mechanics. Journal of Biomechanics 31 (2), 115–123.

Vesely, I., Noseworthy, R., 1992. Micromechanics of the fibrosa and the ventricularis in aortic valve leaflets. Journal of Biomechanics 25 (1), 101–113.

Wineman, A.S., Rajagopal, K.R., 2000. Mechanical Response of Polymers Cambridge. Cambridge University Press, Cambridge.

Woo, S.L.Y., Orlando, C.A., Camp, J.F., Akeson, W.H., 1994. Effects of postmortem storage by freezing on ligament tensile behavior. Journal of Biomechanics 19, 399–404.